Surface & Coatings Technology 316 (2017) 22–29

Contents lists available at ScienceDirect

Surface & Coatings Technology

journal homepage: www.elsevier.com/locate/surfcoat

The investigation of the structures and tribological properties of F-DLC coatings deposited on Ti-6Al-4V alloys

Junjun Wang [a,b], Jianjun Ma [a], Weijiu Huang [a,b,*], Linqing Wang [c], Haoran He [a], Chenglong Liu [a,b]

[a] College of Materials Science and Engineering, Chongqing University of Technology, Chongqing 400054, People' Republic of China
[b] Chongqing Collaborative Innovation Center for Brake Tribological Materials, Chongqing 400054, People' Republic of China
[c] School of Optoelectronic Information, Chongqing University of Technology, Chongqing 400054, People' Republic of China

ARTICLE INFO

Article history:
Received 30 May 2016
Revised 23 January 2017
Accepted in revised form 25 February 2017
Available online 28 February 2017

Keywords:
Ti-6Al-4V alloy
Fluorine doped diamond-like carbon coating
Mechanical property
Tribological property

ABSTRACT

Fluorine doped diamond-like carbon (F-DLC) coatings were deposited on Ti-6Al-4V alloy using a hollow cathode plasma immersion ion implantation deposition system. The aim of this work is to investigate the influence of F content on the surface morphology, structure, mechanical and tribological properties (under air and stroke-physiological saline solution) of the F-DLC coatings. The results reveal that the ratio of H/fE instead of H/E can be well predicting the anti-wear results when the F-DLC coatings have enough adhesion strength, where H is hardness, E is Young's modulus and f is friction coefficient. The F-DLC coatings with high F content exhibit excellent tribological property under air. The low F content F-DLC coatings present super-low friction coefficient and wear rate in stroke-physiological saline solution. Reasons for the tribological property are proposed in combination with the films' morphology and mechanical property.

1. Introduction

Ti-6Al-4V alloy is the most commonly used alloy in the aerospace, automotive, biomedical and other industries due to the excellent mechanical and physical properties, such as high strength to weight ratio, excellent corrosion and biocompatibility. Especially, there are an increasing number of devices being made of titanium alloys [1]. However, in spite of these excellent properties it exhibits poor tribological behavior, a high friction coefficient and large wear loss, limits its application in above mentioned industries [1,2]. Therefore, a lot of attempts have been made by several researchers to overcome the poor tribological behavior in order to broaden its application fields. One of the most well-known methods to improve the tribological behavior of Ti-6Al-4V alloy is to provide a hard and wear resistant coating on the surface using modification techniques [3–11], such as physical vapor deposition and chemical vapor deposition (PVD/CVD), thermal oxidation (TO), ion implantation, micro-arc oxidation.

Diamond-like carbon (DLC) coatings are excellent candidates for use as anti-wear resistant and biocompatible films on biomedical implants due to its extreme mechanical hardness, low coefficient of friction and excellent biocompatibility [12,13]. Although carbon only DLC film is used for a large of applications, the introduction of other elements such as Si, F, N and metals is quite common [14]. In particular, Fluorine doped DLC coatings (F-DLC) have attracted extensive interest because of their low surface energy, chemical inertness, low friction and biocompatibility [15–25]. The major causes for choosing Fluorine as doped element is that incorporation of fluorine can reduce DLC film surface energy, combined with its biocompatibility, it make F-DLC is a promising coating material for biomedical devices, e.g. reducing of bacterial attachment, increasing of antithrombogenicity [16,17,19–21,26]. Another primary reason for choosing Fluorine as doped element is that two F-terminated diamond surfaces sliding against each other would exert higher repulsive forces compared to two H-terminated surfaces, thus, mutual interaction of two F-DLC surfaces would result in a lower COF [27,28]. Even more important, F-DLC films show low COF at high relative humidity atmosphere [29]. However, existing studies rarely dealt with the tribological properties of F-DLC films deposited on Ti-6Al-4V alloy, which is expected to be applicable in the field of medicine.

In our previous work, a novel hollow cathode plasma immersion ion implantation (HCPIII) method was developed. This method takes advantage of plasma ion immersion and high density hollow cathode plasma generated between two parallel-plate electrodes plate, allowing decomposition of precursor and subsequent deposition of *Si*-DLC films [30,31]. In this work we report the synthesis of fluorine doped DLC films by HCPIII technique. The influence of F content on the structure, mechanical properties and surface morphology of DLC coatings was investigated systematically. Optimum deposition parameters for F-DLC coatings with the excellent tribological properties under air and

* Corresponding author.
E-mail address: huangweijiu@cqut.edu.cn (W. Huang).

http://dx.doi.org/10.1016/j.surfcoat.2017.02.065
0257-8972/

Table 1
Deposition conditions for F-DLC films.

Samples	Ar (sccm)	CF_4 (sccm)	C_2H_2 (sccm)	Voltage (kV)	Duty cycle (%)
1	120	–	60	0.9	30
2	120	40	60	0.9	30
3	120	60	60	0.9	30
4	120	90	40	0.9	30

stroke-physiological saline solution (SPSS) were outlined. The findings of this research are of significant reference value for F-DLC films applied in clinical medicine.

2. Experimental details

2.1. Film deposition

Ti-6Al-4V substrates with dimensions 50 × 25 × 10 mm were ground and polished down to Ra = 10 nm using typical metallographic means, and then cleaned ultrasonically in ethanol and acetone baths in succession for 20 min and dried with nitrogen. DLC coatings were deposited using a HCPIII technique. The setup and process with a schematic of HCPIII have been discussed previously [30]. Briefly, after loading the substrates on substrate holder, the chamber was pumped down to a low background pressure less than 2.0×10^{-4} Pa. Before deposition,

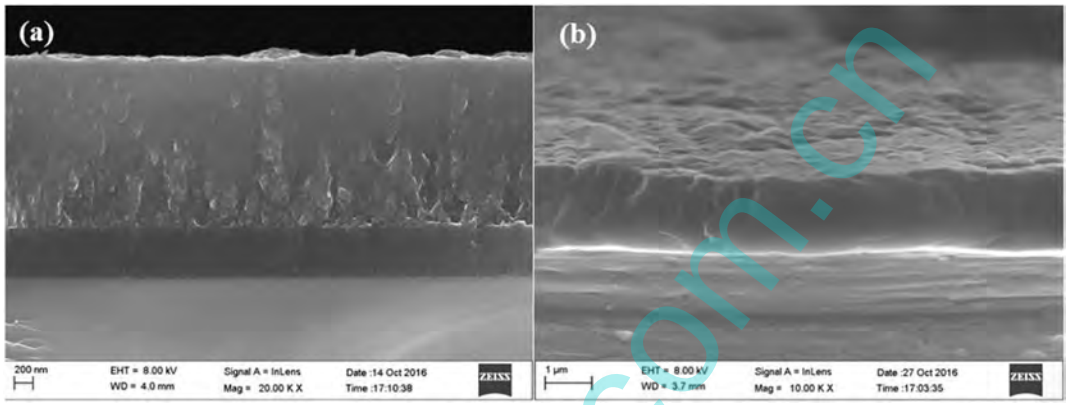

Fig. 1. SEM cross section of the F-DLC film with 3.2 at.% F deposited on (a) Si substrate (b) Ti-6Al-4V substrate.

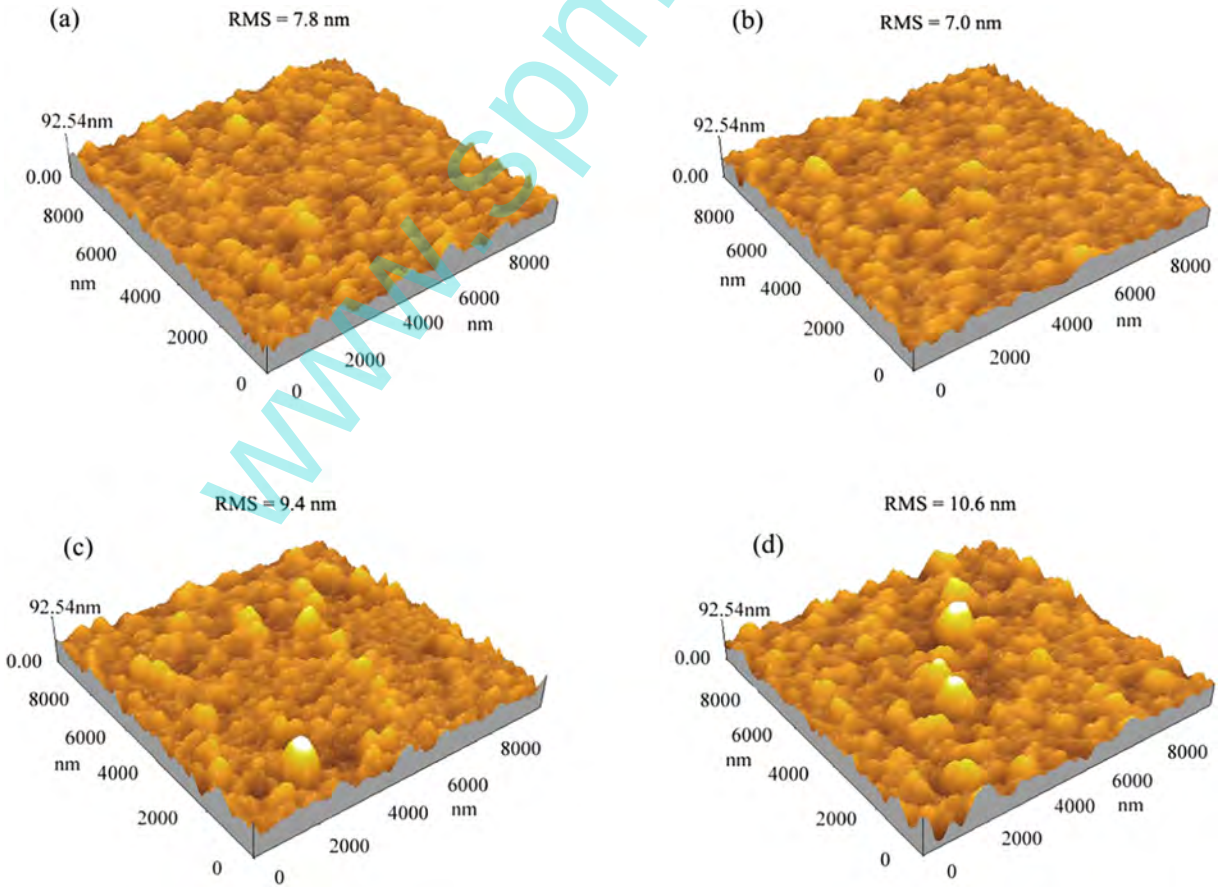

Fig. 2. AFM images of F-DLC films with different F atomic concentration. (a) 0 at.% (b) 3.2 at.% (c)8.3 at.% (d) 16.3 at.%.

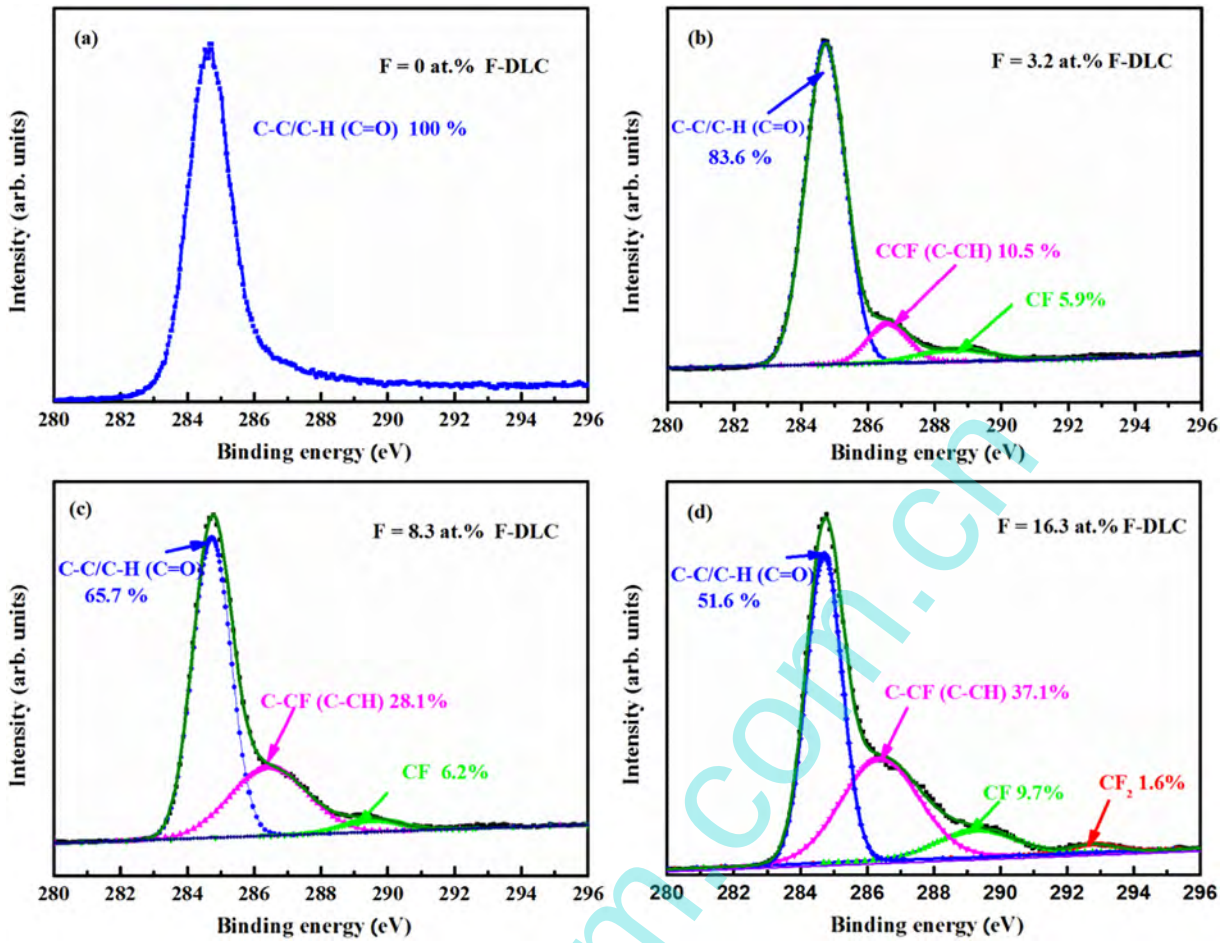

Fig.3. C 1s XPS spectra of the deposited with different F atomic concentration. (a) 0 at.% (b) 3.2 at.% (c)8.3 at.% (d) 16.3 at.%

the substrates were pre-sputtered to remove surface residual contaminants at a pressure of 1.5 Pa for 30 min with Ar plasma. The substrate bias voltage was adjusted to a pulse amplitude of −800 V, a duty cycle of 30%, and a repetition frequency of 1500 Hz. And then, silicon ions were implanted into the substrate from the silane (SiH_4) plasmas for 15 min to increase their adhesion strength between film and substrate, where the substrate bias voltage was changed to a pulse amplitude of −1800 V, a duty cycle of 30%, and a repetition frequency of 1500 Hz. Finally, F-DLC films with varying F contents were deposited by introducing a mix gas of C_2H_2, Ar and CF_4 in vacuum chamber using the parameters listed in Table 1. Effective bias current is in the range of 0.5 to 0.9 A. The total thickness of the F-DLC coatings was about 1.4 μm.

2.2. Film characterizations

The thicknesses of the films were measured by scanning electron microcopy (SEM, Zeiss Sigma) and surface profilometer (Alpha-step IQ, USA). In surface profilometer, a step on coated surfaces was created in order to capture the step profile. The morphologies of specimens were measured with atomic force microscopy (AFM, CSPM4000, Benyuan, China). The chemical composition and bonding states of the film were determined by X-ray photoelectron spectroscopy (XPS, PHI-5700) with unmonochromatized Mg Ka radiation ($h\nu = 1253.6$ eV). C1s and F1s XPS spectra of F-DLC film samples were recorded every 1 eV. Raman spectra were obtained using a Renishaw 2000 micro-Raman system. Laser wavelength and grating is 532 nm and 1800 line/nm, respectively. The diameter of the laser spot was 2.5 μm. The scanning range was 800–3000 cm^{-1}. The internal stress measured by FST-1000 type film stress tester. In specially, specimens were cut into 25 × 25 mm pieces and the curvature of the film/substrate before (R_0) and after film deposition (R) was measured. The value of internal stress was calculated from the curvature of film/substrate using the Stoney equation [32].

$$\sigma = \frac{1}{6}\frac{E_s}{1-v_s}\left(\frac{1}{R}-\frac{1}{R_0}\right)\frac{t_s^2}{t_f}$$

where E_s is Young's modulus, ν_s is Poisson's ratio and t_s and t_f is the thickness of the substrate and the coated film, respectively. The hardness and elastic modulus of the films were determined by the Oliver-Pharr method using a calibrated Hysitron Triboindenter with a diamond Berkovich tip. All nanoindentation tests were performed with the tip penetration depth of around 10% of the film thickness. Six repeated measurements were made for each specimen. The adhesion of the sample was tested by a scratch tester (CSEM Revetest) equipped with a diamond tip of radius 200 μm. The normal load was increased from 0 to 30 N at a loading rate of 30 N/min and a scratching speed of 5 mm/min. During the scratch test friction force was continuously monitored. The tribological performances of the specimen were investigated with a ball on disc tester. The counterpart was hardened (HRC 60-62) GCr 15 steel ball with a diameter of 6 mm. The tests were performed at 1.6 mm/s speed under air (temperature of about 37 ± 2 °C, and a relative humidity of 20%–30%) or SPSS (temperature of about 37 ± 2 °C) in

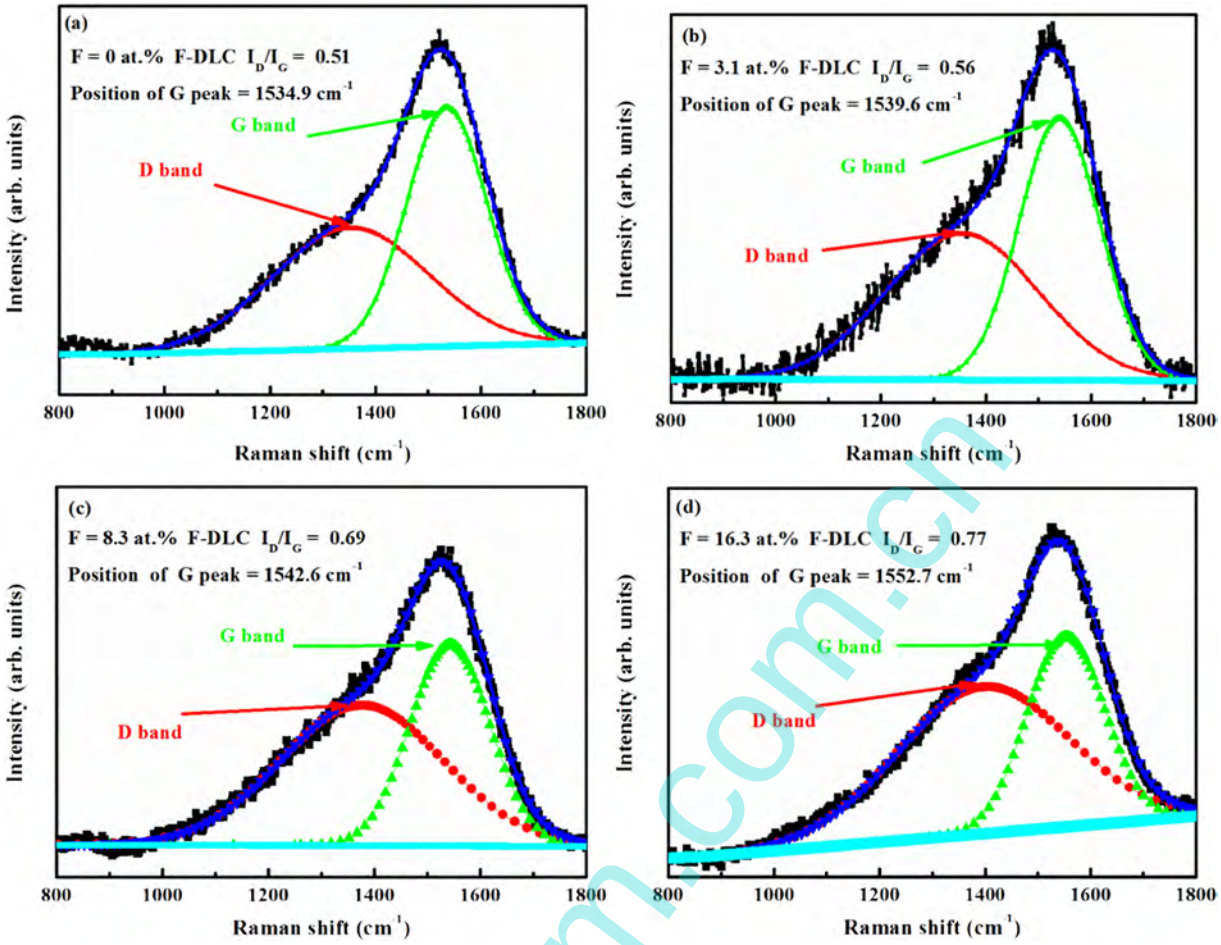

Fig. 4. Decomposition of Raman spectra for F-DLC films as a function of F content. (a) 0 at.% (b) 3.2 at.% (c)8.3 at.% (d) 16.3 at.%.

which a constant load (5 N) was applied for 60 min. A non-contact 3D surface profiler (model MicroMAXTM, USA) was used to capture images on a wear track for measuring the wear volume. The wear rate of the films was defined as the volume of removed material at a unit load and in a unit sliding distance. Five profilometry traces were taken on each wear surface to measure wear depths and cross-sectional areas.

3. Results and discussion

Fig. 1 shows the cross-section of the F-DLC film deposited on Si and Ti64 substrate. It is clear that the film presents multilayered structure including a Si interlayer and a DLC top layer, the total thickness is about 1.6 μm. Moreover, the F-DLC is uniformed and it well adheres to

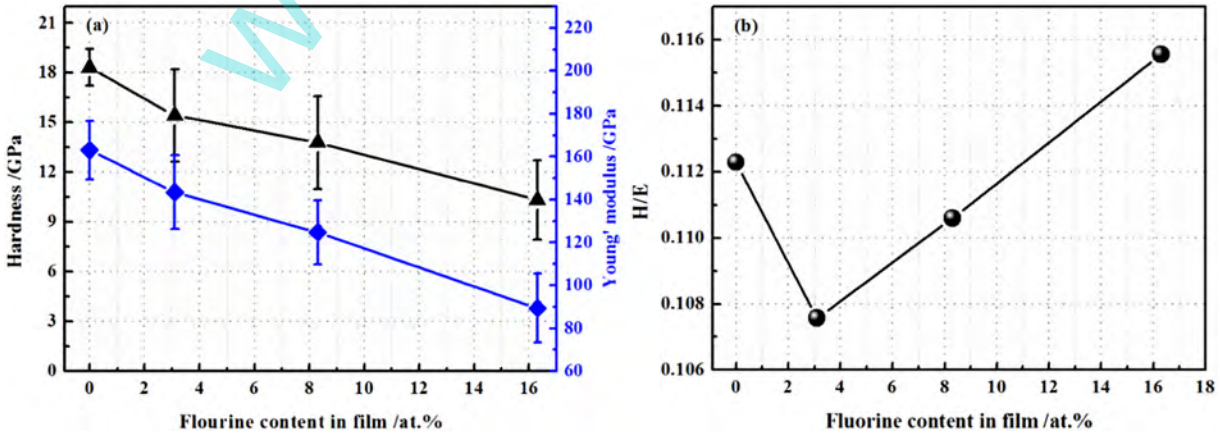

Fig. 5. (a) Hardness and elastic modulus and (b) H/E ratio of the F-DLC films as function of F contents. Reported values and error bars represent averages and standard deviations, respectively, based on six different measurements on each of films.

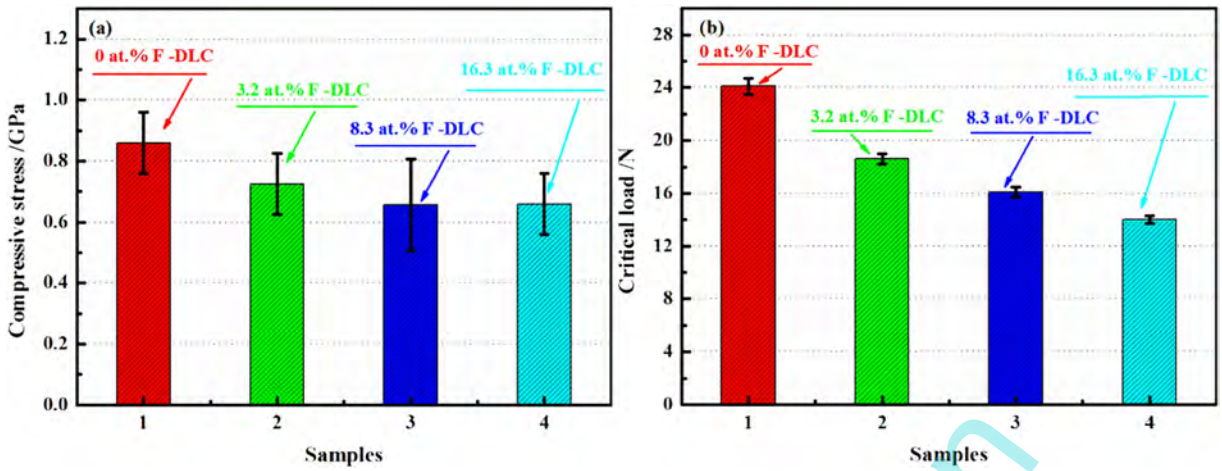

Fig. 6. (a) Compressive stress and (b) critical load of F-DLC as a function of the F content. Reported values and error bars represent averages and standard deviations, respectively, based on three different measurements on each of prepared films.

substrate. AFM images of F-DLC films are given as shown in Fig.2. It is found that no large particles and obvious defects are observed on all as-prepared films. The surface roughness increase with increase in F content (3.2 to 16.3 at.%). The root-mean-squared roughness (RMS) of 0, 3.2, 8.3 and 16.3 at.% F-DLC film is 7.8, 7.0, 9.4 and 10.6 nm, respectively. It is known that the growth of DLC films depend on the competition between deposition and etching. As the CF_4 increases in the plasma, the density of -CF_x groups and F^+ increases. The F^+ is an efficient etching agent which leads to a smoothed surface [33]. However, the kinetic energy of the ions decreases as the same time. As a result, low energy ion doesn't have enough energy to remove certain asperities resulting in a rougher film surface [34].

The chemical structure of the F-DLC films with different F content was examined by XPS. The fluorine content was calculated by the following equation:

$$\text{atomic concentration}\ (\%) = \frac{A_i/S_i}{\sum_i (A_i/S_i)}$$

where subscript is film element, A and S is the peak area and sensitivity factor of the element (S = 0.78, 1 for C 1s and F 1s) [14]. The calculation results show that the fluorine content increases from 0 to 16.3 at. % as the ratio of CF_4 and C_2H_2 increases. Fig. 2 shows the C1s XPS spectra for each F-DLC film surface. At a relatively low F content, 3.2 and 8.3 at.% F in DLC, the C1s spectrum of the F-DLC film is well deconvoluted into three Gaussian peaks corresponding to CF (289.2 eV), C-CF (286.3 eV), and C-C/C-H (284.7 eV). However, another bonding state, CF_2 (292.4 eV) appears in the F-DLC film when F content increase to 16.3 at.%. The bond concentration according to the relevant peak area divided by the sum of all the peaks area is also presented in Fig. 3. It is clear that the bond concentration of C-C/C-H bonding state decrease sharply. Concentration of C—C bonding for 0, 3.1, 8.3 and 16.3 at.% F-DLC is about 100, 83.6, 65.7 and 51.6%, respectively. While the -C-CF and CF bonding state increase evidently with rising F content in DLC film from 0 at.% to 16.3 at.%.

It is well known that a typical Raman spectrum of DLC is composed of G and D bands, in which the G band centered approximately at 1550 cm^{-1} is due to the symmetric E_{2g} vibrational mode in graphite-like materials and the D band at approximately 1330 cm^{-1} comes from the limitations in the graphite domain size induced by grain boundaries or imperfections [35]. For the sake of revealing the evolution of microstructure of F-DLC with various F content, peak position of all the Raman spectra were determined by Gaussian fitting in the 800–1800 cm^{-1} region as shown in Fig. 4. It is evident that all the films show typical characters of DLC. Quantitative analysis of Raman spectrum show that the intensity ratio of D and G band (I_D/I_G) increases with increasing F content. The intensity ratio of D peak and G peak I_D/I_G are 0.51, 0.56, 0.69 and 0.77, corresponding to F content of 0, 3.2, 8.3 and 16.3 at.%, respectively. The relevant G band peak central positions are located at 1534.9, 1539.6, 1542.6 and 1552.7 cm^{-1}, which have an upshift tendency. This indicates the sp^3/sp^2 ratio decreases and films became more graphitic. A similar trend is reported also in other studies [24,36,37]. In addition, increasing luminescence intensity was observed for higher fluorine concentrations (16.3 at.%), which could be assigned to a polymer like structural arrangement. Yao et al. [37] suggested that the cross-linked C—C bond in DLC film would be broken and the sp^3 diamond-like matrix would be collapsed when fluorine was introduced in film, so and the sp^2 carbon domains increases in the fluorinated films. Gueorguiev et al. [38] pointed out that F and C could only form a single bond, the formed C—F stick out of the C—C network and disrupted the local carbon microstructure by reducing the formation of large rings and chains. As a result, the sp^3 transform to sp^2. With increasing F concentration, the large rings continue to grow up and accelerated the interlocking of rings at the edge of the C—C network, leading the formation of polymer-like structures. Therefore, we can conclude that incorporation F into DLC film decrease the sp^3/sp^2

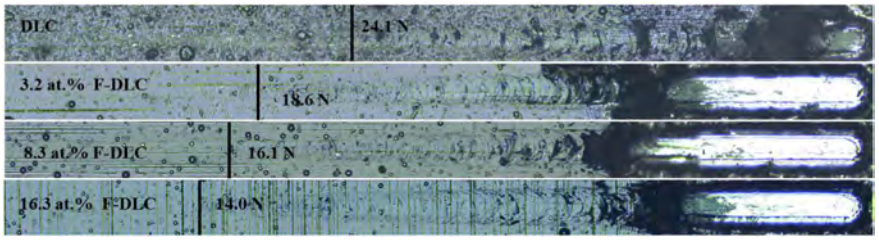

Fig. 7. Optical image of F-DLC films scratch track with different F content.

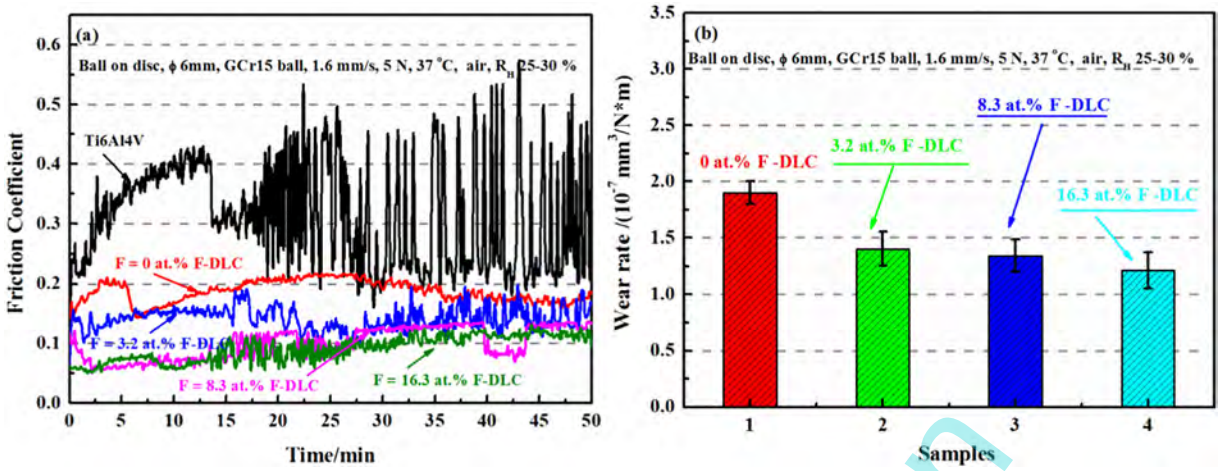

Fig. 8. (a) Friction coefficient and (b) wear rate of F-DLC film with different F concentration in ambient air environment. Reported values and error bars of wear rate represent averages and standard deviations, respectively, based on five different measurements on each of prepared films.

ratio and create more polymer like structural arrangement in the DLC film.

The hardness and Young's modulus of the films as a function of the fluorine content in the films are presented in Fig. 5 (a). Given that the maximum penetration depth is less than 1/10 of film thickness avoiding the effect of the substrate material. Reported values and error bars represent averages and standard deviations, respectively, based on five different measurements on each of prepared films. It is noted that both the hardness and Young' modulus of the films decreases with increasing F content in films. The harness for 0, 3.2, 8.3 and 16.3 at.% F-DLC is 18.3, 15.4, 13.8, 10.3 GPa, respectively. The Young's modulus of the film decreases from 163.2 GPa (0 at.% F-DLC) to 89.4 GPa (16.3 at.% F-DLC). Yao et al. [37] attributed the decrease in the hardness and Young's modulus to the C—F formation, because the C—F bonds weaker than C═C bonds. Jacobsohn et al. [39] suggest that the hardness of the DLC films is given by C-C network, which will be locally interrupted by F. Introduction of F decreases cross-linking creates a new and more open structural arrangement leading to lower hardness and Young's modulus. H/E ratio, a helpful parameter for predicting wear resistance [40], is plotted in Fig. 5 (b) as a function of F percentage in the F-DLC film. It is clear that the H/E with the F content first decreases and then increases. The H/E reaches the minimum 0.107 when the F percentage in film is 3.2 at.%.

Internal stress was compressive in all tested samples and the measured values are plotted in Fig. 6 (a) as a function of the fluorine percentage in the coating. Reported values and error bars represent averages and standard deviations, respectively, based on three different measurements on each of prepared films. It is note that the compressive stress decreases monotonically with increasing F concentration. Comparing the stress values obtained for DLC without F (0.86 GPa) and F-DLC with 13.2 at.% F, an internal stress reduction about 0.2 GPa is achieved. The reduction of compressive stress is correlated with the bonding structure. The incorporation of F atoms into the DLC gives rise to the formation of HF volatile gas, which reduces the content of hydrogen, especially, the unbound hydrogen. It has been found that the reduction of unbound hydrogen leads to decreases in volume and strain, thus decreasing the residual stress [41]. Furthermore, it is believe that the sum of F and H contents is nearly constant in F-DLC film. Because F atom has bigger dimensions than H atom, introduction F in DLC lower the atomic density by replacing hydrogen, thus the stiffness of the carbon network decreases and the internal stress reduces [33,42]. Fig. 6 (b) shows the critical load as a function of F content. It is clear that the higher F content film has a lower critical load than that of the lower F content film. The maximum critical load for pure DLC film is about 24.1 N. The minimum critical load is about 14.0 N for 16.3 at.% F-DLC. This is probably low F content DLC films have higher hardness, which leads the difficulty of diamond stylus penetration in the film. The morphologies of the scratch tracks are presented in Fig. 7.

The friction coefficient of F-DLC film with different F concentrating measured by a ball on disk tribological tester under ambient air is shown in Fig. 8 (a). The sliding speed and the loading are 1.6 mm/s and 5 N, respectively. The temperature is about 37 °C and the relatively humidity is 25–30%. By contrast, friction coefficient of substrate is also presented. It is note that Ti6Al4V exhibits a high, fluctuating friction coefficient within the range of 0.16 and 0.5. For these F-DLC tests, the tribometry results show that all films run in to a low friction value (0.05–0.21). Moreover, the friction decreases with increasing F content. The steady friction coefficient of 0, 3.2, 8.3 and 16.3 at.% F-DLC is about 0.18, 0.15, 0.13 and 0.11, respectively. Fig. 8 (b) provides the wear rate of F-DLC film with different F content. It can be seen that there are clear correlations between the F content and the wear rate. The wear rate decreases with increase in F in F-DLC film. The lowest wear rate of 1.2×10^{-7} mm^3/N * m is achieved on the F-DLC film with 16.3 at.% F content. This changing trend may relate to their mechanical property. The ratio between H and E also called 'plasticity index' is widely quoted as a valuable measure in determining the limit of elastic behavior in a surface contact and is provided extremely close agreement to their ranking in terms of wear. The higher the H/E ratio, the better the materials' wears resistance [40]. However, some contradiction is appeared in

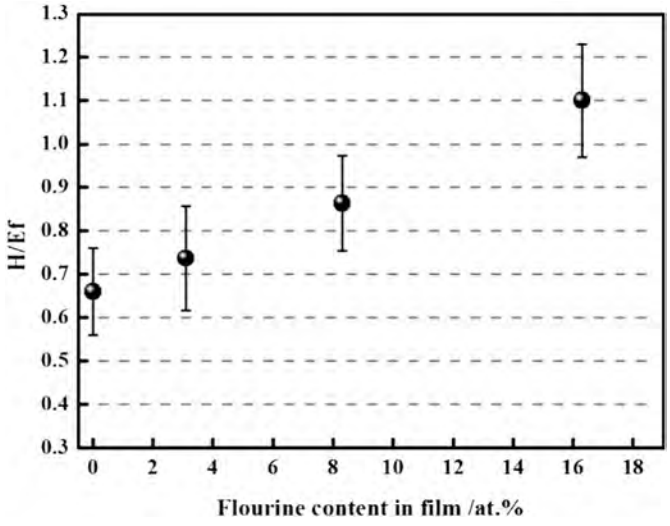

Fig. 9. The H/(Ef) value of F-DLC films with different F content.

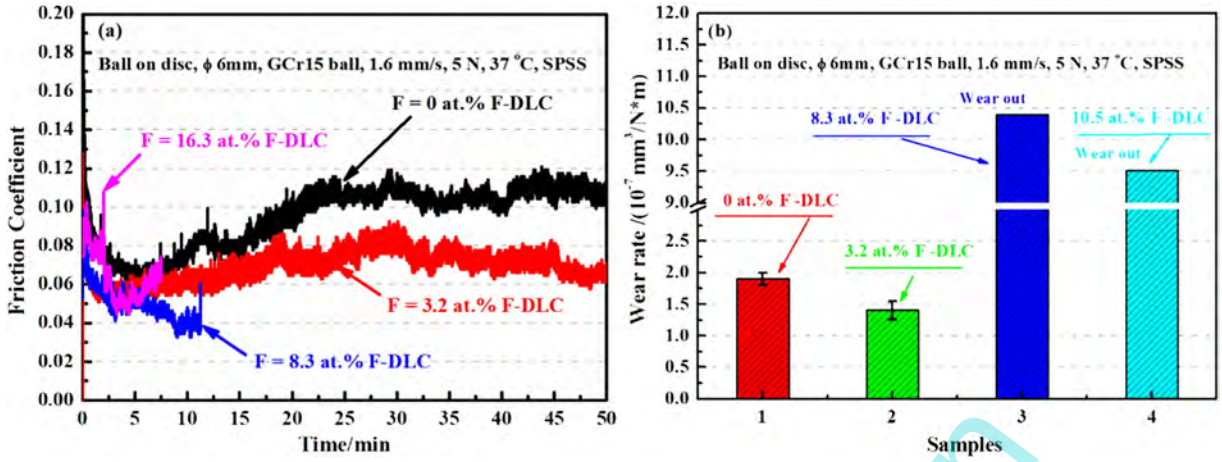

Fig. 10. (a) Friction coefficient and (b) wear rate of F-DLC film in SPSS. The sliding speed, the loading and the temperature are 1.6 mm/s, 5 N, and 37 °C, respectively. Reported values and error bars of wear rate represent averages and standard deviations, respectively, based on at least three measurements on each of the films.

study. The H/E decrease first and then increase. It reaches the minimum value of 0.107 when the F percentage in film is 3.2 at.%. But the corresponding wear rate value is not the highest. Neuville et al. [43]suggested that the H/E criterion would not predict the superior anti-wear results of polished diamond and ta-C coatings, that the criterion H/Ef would be well predicting the anti-wear results almost all coating materials, where f is the steady state friction coefficient. In this view, surface micro rugosity and the surface chemistry which influence the coating friction coefficient are considered. Fig. 9 shows the H/(Ef) value of F-DLC films with different F content. The H/(Ef) value increases with increasing F content. Compared with the wear rate (Fig. 8(b)), it can be seen that the wear rate of F-DLC film decrease with increasing H/(Ef). So we can conclude that the criterion H/fE will be well predicting the anti-wear results.

Fig. 10 (a) shows the dynamic evolution of coefficient of friction of F-DLC films with different F content in SPSS. It can clear that the films present low friction coefficient, within the range of 0.04 and 0.11. For low F content F-DLC films, friction coefficient quickly decrease to a low value at first, thereafter slowly grew is observed and a steady state is reached at the end of test. The steady state value of friction coefficient is around 0.11 and 0.07 for the 8.3 and 16.3 at.% F-DLC films, respectively. However, it is observed that F-DLC films with high F content fail easily during tests in spite of the low friction coefficient compared with the low F films. Wearing life under this study imposed sliding conditions is only 7 and 12 min for 8.3 and 16.3 at.% F-DLC films, respectively. The wear rate of the F-DLC films in SPSS is summarized in Fig. 10 (b). The wear rate of pure DLC film and 3.2 at.% F-DLC film are 1.9×10^{-7} and 1.4×10^{-7} $mm^3/N * m$, respectively. F-DLC films with 8.3 and 16.3 at.% is worn out. Fig. 11 shows the wear track morphologies of 0 and 3.2 at.% F-DLC film. It is clear that several unexpected partial delaminations and cracking are observed within the film wear track without F. However, the wear track of 3.2 at.% F-DLC just shows some NaCl particles (confirmed by EDS) and some small pieces of film being peeled off of the substrate. Different tribological behavior is maybe attributed to the roughness of F-DLC films. High RMS of F-DLC with high F content allowing more saline solution into the gap between surface microbulge. Addition contact stress is generated due to "wedge effect" at the start of the tribological test, which leads to a rapid deterioration of the contacting surfaces [15].

In this study, the F-DLC film with 3.2 at.% F exhibits excellent tribological property, especially in SPSS. However, in order to expand F-DLC application in medical devices, further investigations on the biocompatibility and corrosion resistance needed to be conducted.

4. Conclusions

Fluorine doped DLC (F-DLC) coating was deposited on Ti-6Al-4V alloy using a hollow cathode plasma immersion ion implantation deposition system. The morphologies of specimens were measured with AFM. The structures and chemical bonding was examined by Raman and X-ray photoelectron spectroscopy techniques. Mechanical and tribological properties were evaluated using nanoindentation, scratch and ball-on-disk sliding friction testing. The major results are drawn as follows:

(1) The surface roughness of the F-DLC film with high F content is rougher than that of the undoped DLC film and RMS increases with increase F percentage in the film.

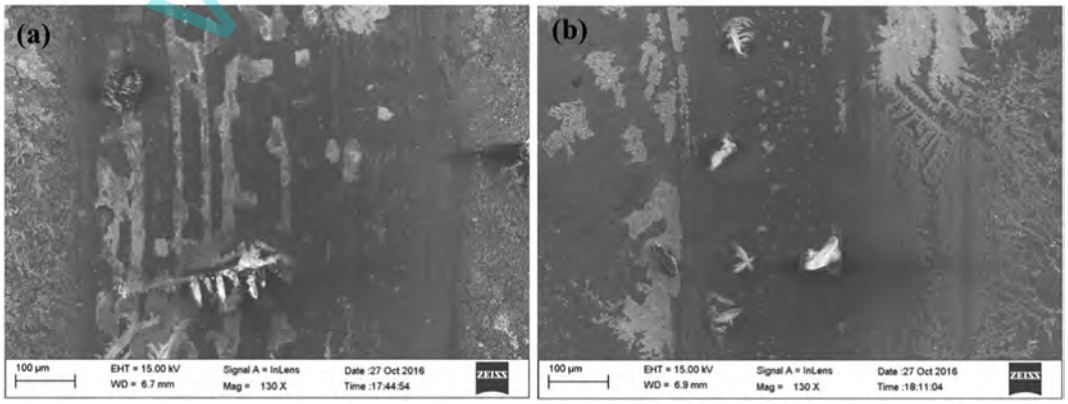

Fig. 11. SEM surface morphologies on a worn track of F-DLC film with different F content in SPSS. (a) 0 at.% (b) 3.2 at.%

(2) Both the hardness and Young' modulus of the films decreases with increasing F content in films The H/E reached the minimum 0.107 when the F percentage in film was 3.2 at.%.
(3) The friction decreases with increasing F content in air, the criterion H/fE will be well predicting the anti-wear results when the F-DLC films have enough adhesion strength.
(4) Lower F content F-DLC coating present super-low friction coefficient and wear rate in SPSS. The possible reasons are that it has lowest RMS.

Acknowledgements

This work was supported by the Natural Science Foundation of China (Grant No. 51505050), the Major Application Development Project in Chongqing, China (Grant No. cstc2014yykfC50002), Basic and Frontier Research Program of Chongqing, China (Grant No. cstc2013jjB50003) and the Scientific and Technological Research Program of Chongqing Municipal Education Commission, China (Grant No. KJ1500910, KJ1500942).

References

[1] M. Geetha, A.K. Singh, R. Asokamani, A.K. Gogia, Ti based biomaterials, the ultimate choice for orthopaedic implants – a review, Prog. Mater. Sci. 54 (2009) 397–425.
[2] D.V. Shtansky, M. Roy, Surface engineering for biotribological application, in: M. Roy (Ed.), Surface Engineering for Enhanced Performance Against Wear, Springer, Vienna 2013, pp. 277–310.
[3] W. Pawlak, K.J. Kubiak, B.G. Wendler, T.G. Mathia, Wear resistant multilayer nanocomposite WC1 − x/C coating on Ti–6Al–4V titanium alloy, Tribol. Int. 82 (Part B) (2015) 400–406.
[4] M. Jelinek, T. Kocourek, J. Zemek, J. Mikšovský, Š. Kubinová, J. Remsa, J. Kopeček, K. Jurek, Chromium-doped DLC for implants prepared by laser-magnetron deposition, Mater. Sci. Eng. C 46 (2015) 381–386.
[5] S. Wang, Z. Liao, Y. Liu, W. Liu, Different tribological behaviors of titanium alloys modified by thermal oxidation and spraying diamond like carbon, Surf. Coat. Technol. 252 (2014) 64–73.
[6] A. Escudeiro, T. Polcar, A. Cavaleiro, a-C(:H) and a-C(:H)_Zr coatings deposited on biomedical Ti-based substrates: tribological properties, Thin Solid Films 538 (2013) 89–96.
[7] F. Casadei, M. Tului, Combining thermal spraying and PVD technologies: a new approach of duplex surface engineering for Ti alloys, Surf. Coat. Technol. 237 (2013) 415–420.
[8] J.B. Cai, X.L. Wang, W.Q. Bai, X.Y. Zhao, T.Q. Wang, J.P. Tu, Bias-graded deposition and tribological properties of Ti-contained a-C gradient composite film on Ti6Al4V alloy, Appl. Surf. Sci. 279 (2013) 450–457.
[9] C. Martini, L. Ceschini, B. Casadei, I. Boromei, J.B. Guion, Dry sliding behaviour of hydrogenated amorphous carbon (a-C:H) coatings on Ti-6Al-4V, Wear 271 (2011) 2025–2036.
[10] X. Guan, Z. Lu, L. Wang, Achieving high tribological performance of graphite-like carbon coatings on Ti6Al4V in aqueous environments by gradient Interface design, Tribol. Lett. 44 (2011) 315–325.
[11] D.G. Bansal, O.L. Eryilmaz, P.J. Blau, Surface engineering to improve the durability and lubricity of Ti–6Al–4V alloy, Wear 271 (2011) 2006–2015.
[12] K. Bewilogua, D. Hofmann, History of diamond-like carbon films — from first experiments to worldwide applications, Surf. Coat. Technol. 242 (2014) 214–225.
[13] J. Robertson, Diamond-like amorphous carbon, Mater. Sci. Eng. R. Rep. 37 (2002) 129–281.
[14] J.C. Sánchez-López, A. Fernández, Doping and alloying effects on DLC coatings, in: C. Donnet, A. Erdemir (Eds.), Tribology of Diamond-like Carbon Films: Fundamentals and Applications, Springer US, Boston, MA 2008, pp. 311–338.
[15] R. Ismail, Running-in of Rolling-Sliding Contacts, Enschede, 2013 152.
[16] D.W. Ren, Q. Zhao, A. Bendavid, Anti-bacterial property of Si and F doped diamond-like carbon coatings, Surf. Coat. Technol. 226 (2013) 1–6.
[17] G. Prihandana, I. Sanada, H. Ito, M. Noborisaka, Y. Kanno, T. Suzuki, N. Miki, Antithrombogenicity of fluorinated diamond-like carbon films coated nano porous polyethersulfone (PES) membrane, Materials 6 (2013) 4309–4323.
[18] L. Nobili, A. Guglielmini, Thermal stability and mechanical properties of fluorinated diamond-like carbon coatings, Surf. Coat. Technol. 219 (2013) 144–150.
[19] A. Jiang, J. Xiao, X. Li, Z. Wang, Effect of structure, composition, and micromorphology on the hydrophobic property of F-DLC film, J. Nanomater. 2013 (2013) 1–7.
[20] T. Hasebe, S. Nagashima, A. Kamijo, M.-W. Moon, Y. Kashiwagi, A. Hotta, K.-R. Lee, K. Takahashi, T. Yamagami, T. Suzuki, Hydrophobicity and non-thrombogenicity of nanoscale dual rough surface coated with fluorine-incorporated diamond-like carbon films: biomimetic surface for blood-contacting medical devices, Diam. Relat. Mater. 38 (2013) 14–18.
[21] C.-C. Chou, Y.-Y. Wu, J.-W. Lee, C.-H. Yeh, J.-C. Huang, Characterization and haemocompatibility of fluorinated DLC and Si interlayer on Ti6Al4V, Surf. Coat. Technol. 231 (2013) 418–422.
[22] C.-C. Chou, Y.-Y. Wu, J.-W. Lee, J.-C. Huang, C.-H. Yeh, Mechanical properties of fluorinated DLC and Si interlayer on a Ti biomedical alloy, Thin Solid Films 528 (2013) 136–142.
[23] C. Jongwannasiri, N. Moolsradoo, A. Khantachawana, P. Kaewtatip, S. Watanabe, The comparison of biocompatibility properties between Ti alloys and fluorinated diamond-like carbon films, Adv. Mater. Sci. Eng. 2012 (2012) 1–8.
[24] M.H. Ahmed, J.A. Byrne, J. McLaughlin, Evaluation of glycine adsorption on diamond like carbon (DLC) and fluorinated DLC deposited by plasma-enhanced chemical vapour deposition (PECVD), Surf. Coat. Technol. 209 (2012) 8–14.
[25] K. Kanda, N. Yamada, K. Yokota, M. Tagawa, M. Niibe, M. Okada, Y. Haruyama, S. Matsui, Fabrication of fluorine-terminated diamond-like carbon thin film using a hyperthermal atomic fluorine beam, Diam. Relat. Mater. 20 (2011) 703–706.
[26] H.-C. Cheng, S.-Y. Chiou, C.-M. Liu, M.-H. Lin, C.-C. Chen, K.-L. Ou, Effect of plasma energy on enhancing biocompatibility and hemocompatibility of diamond-like carbon film with various titanium concentrations, J. Alloys Compd. 477 (2009) 931–935.
[27] F.G. Sen, Y. Qi, A.T. Alpas, Tribology of fluorinated diamond-like carbon coatings: first principles calculations and sliding experiments, Lubr. Sci. 25 (2013) 111–121.
[28] S. Bhowmick, F.G. Sen, A. Banerji, A.T. Alpas, Friction and adhesion of fluorine containing hydrophobic hydrogenated diamond-like carbon (F-H-DLC) coating against magnesium alloy AZ91, Surf. Coat. Technol. 267 (2015) 21–31.
[29] M. Rubio-Roy, C. Corbella, E. Bertran, S. Portal, M.C. Polo, E. Pascual, J.L. Andújar, Effects of environmental conditions on fluorinated diamond-like carbon tribology, Diam. Relat. Mater. 18 (2009) 923–926.
[30] J. Wang, J. Pu, G. Zhang, L. Wang, Interface architecture for superthick carbon-based films toward low internal stress and ultrahigh load-bearing capacity, ACS Appl. Mater. Interfaces 5 (2013) 5015–5024.
[31] J. Wang, J. Pu, G. Zhang, L. Wang, Tailoring the structure and property of silicon-doped diamond-like carbon films by controlling the silicon content, Surf. Coat. Technol. 235 (2013) 326–332.
[32] B.R. Lawn, T.R. Wilshaw, J.R. Rice, Fracture of brittle solids (Cambridge solid state science series), J. Appl. Mech. 44 (1977).
[33] S. Samukawa, T. Mukai, Differences in radical generation due to chemical bonding of gas molecules in a high-density fluorocarbon plasma: effects of the C = C bond in fluorocarbon gases, J. Vac. Sci. Technol. A 17 (1999) 2463–2466.
[34] A. Bendavid, P.J. Martin, L. Randeniya, M.S. Amin, The properties of fluorine containing diamond-like carbon films prepared by plasma-enhanced chemical vapour deposition, Diam. Relat. Mater. 18 (2009) 66–71.
[35] A. Ferrari, J. Robertson, Resonant Raman spectroscopy of disordered, amorphous, and diamond-like carbon, Phys. Rev. B 64 (2001).
[36] G.Q. Yu, B.K. Tay, Z. Sun, L.K. Pan, Properties of fluorinated amorphous diamond like carbon films by PECVD, Appl. Surf. Sci. 219 (2003) 228–237.
[37] Z.Q. Yao, P. Yang, N. Huang, H. Sun, J. Wang, Structural, mechanical and hydrophobic properties of fluorine-doped diamond-like carbon films synthesized by plasma immersion ion implantation and deposition (PIII–D), Appl. Surf. Sci. 230 (2004) 172–178.
[38] C. Goyenola, S. Stafström, S. Schmidt, L. Hultman, G.K. Gueorguiev, Carbon fluoride, CFx: structural diversity as predicted by first principles, J. Phys. Chem. C 118 (2014) 6514–6521.
[39] L.G. Jacobsohn, S.S. Camargo Jr., F.L. Freire Jr., Fluorinated a-C:H films investigated by thermal-induced gas effusion, Diam. Relat. Mater. 11 (2002) 1831–1836.
[40] A. Leyland, A. Matthews, On the significance of the H/E ratio in wear control: a nanocomposite coating approach to optimised tribological behaviour, Wear 246 (2000) 1–11.
[41] S. Kumar, D. Sarangi, P.N. Dixit, O.S. Panwar, R. Bhattacharyya, Diamond-like carbon films with extremely low stress, Thin Solid Films 346 (1999) 130–137.
[42] L. Zhang, F. Wang, L. Qiang, K. Gao, B. Zhang, J. Zhang, Recent advances in the mechanical and tribological properties of fluorine-containing DLC films, RSC Adv. 5 (2014) 9635–9649.
[43] S. Neuville, Quantum electronic mechanisms of atomic rearrangements during growth of hard carbon films, Surf. Coat. Technol. 206 (2011) 703–726.